PROCEEDINGS OF SCIENCE

The LHCb RICH Upgrade: Operations and Performance

Federica Borgato[a,b,c,*] **on behalf of the LHCb RICH collaboration**

[a] *Dipartimento di Fisica dell'Università di Padova, Padova, Italy*
[b] *INFN, Sezione di Padova, Padova, Italy*
[c] *European Organization for Nuclear Research (CERN), Geneva, Switzerland*

E-mail: federica.borgato@cern.ch

The LHCb experiment is designed for precision measurements of CP violation and rare decays of beauty and charm hadrons. A key component enabling these studies is the Ring Imaging Cherenkov (RICH) system, which provides robust particle identification (PID) over a wide momentum range. With the start of Run 3 and the transition to a software-based trigger at 40 MHz, the RICH detectors have undergone a major upgrade to meet the new data-taking and performance demands. This contribution presents the design, implementation, and commissioning of the upgraded RICH system. Key features include the replacement of the Hybrid Photon Detectors with new multi-anode photomultiplier tubes (MaPMT), the development of custom readout electronics capable of handling the increased data rate, and the re-optimization of the optical layout to maintain PID performance despite a reduced material budget. Performance metrics such as PID efficiency and stability under high occupancy conditions will be presented, demonstrating that the upgraded RICH system is fully equipped to support the LHCb physics program throughout Run 3.

The European Physical Society Conference on High Energy Physics (EPS-HEP2025)
7-11 July 2025
Marseille, France

*Speaker

© Copyright owned by the author(s) under the terms of the Creative Commons
Attribution-NonCommercial-NoDerivatives 4.0 International License (CC BY-NC-ND 4.0).
All rights for text and data mining, AI training, and similar technologies for commercial purposes, are reserved.
ISSN 1824-8039. Published by SISSA Medialab.

PoS(EPS-HEP2025)518

1. Introduction

The LHCb experiment at CERN's Large Hadron Collider (LHC) is designed to search for new physics beyond the Standard Model by studying b and c quark decays. It operates as a single arm forward spectrometer covering the pseudorapidity range of $2 < \eta < 5$, and is equipped with advanced tracking and particle identification detectors optimized for detecting c- and b-hadrons.

During LHC Run 1 and Run 2, the LHCb experiment operated successfully, achieving excellent performance [1]. Despite these results, the precision of several key flavour-physics observables remained statistically limited, motivating the need for larger datasets to match the accuracy of theoretical predictions and to probe potential new-physics effects [2]. To exploit the higher luminosity foreseen in future runs, it became essential to adopt a new, fully software-based trigger strategy, which, together with the increased luminosity and pile-up, required a comprehensive upgrade of the sub-detectors, front-end electronics, and data-processing software. The upgraded LHCb detector has been designed to operate at an instantaneous luminosity of $L = 2 \times 10^{33}\,\mathrm{cm}^{-2}\,\mathrm{s}^{-1}$, and to read out events at the full LHC bunch-crossing rate of 40 MHz.

Regarding the LHCb RICH sub-detectors, to preserve the performance levels achieved during Run 1 and Run 2 [3], major modifications were implemented. The system was re-optimized to improve Cherenkov-angle resolution and photon yield, accounting for chromatic dispersion, emission-point uncertainty, and sensor granularity. The entire photon-detection chain was replaced to ensure compatibility with the 40 MHz readout architecture. The commissioning and optimization of the Upgrade I RICH sub-detectors is described in the following sections.

2. The LHCb RICH sub-detectors

The RICH system includes two sub-detectors: RICH 1, located closest to the interaction point, covers the momentum range 2 to 50 GeV/c, while RICH 2, positioned after the tracking system, covers the range 15 to 100 GeV/c. These detectors utilize C_4F_{10} and CF_4 gas radiators, respectively, to generate Cherenkov photons, which are focused by mirror systems onto single-photon-sensitive detectors. During Runs 1 and 2 both RICH detectors were equipped with arrays of Hybrid Photon Detectors (HPDs) with embedded 1 MHz readout front-end electronics to match the 1 MHz hardware trigger. For the LHCb RICH Upgrade I detectors, Multianode Photomultiplier Tubes (MaPMT) were selected as the optimal photon sensors, as they satisfy all the required specifications. They enable single-photon detection at the 40 MHz LHC bunch-crossing rate, thanks to their low intrinsic dead time and their coupling with the CLARO ASIC [4]. The devices can sustain detection rates of about $100\,\mathrm{MHz\,cm}^{-2}$ due to their large active area (approximately 80%) and fine spatial granularity (around $10\,\mathrm{mm}^2$), which reduce inefficiencies and mitigate pixel-size effects, facilitating the separation of overlapping Cherenkov rings. Their gain is about 10^6 electrons and their quantum efficiency is approximately 30% at 300 nm, thus maximising the photon yield per charged particle and with a spectral range that limits chromatic dispersion. In addition, MaPMT exhibit a low dark-count rate of about $10\,\mathrm{kHz/cm}^2$ and minimal intrinsic electronic noise, ensuring stable and reliable operation. An accumulated photon hitmap on the detector planes for both RICH 1 and RICH 2 can be seen in Figure 1.

PoS(EPS-HEP2025)518

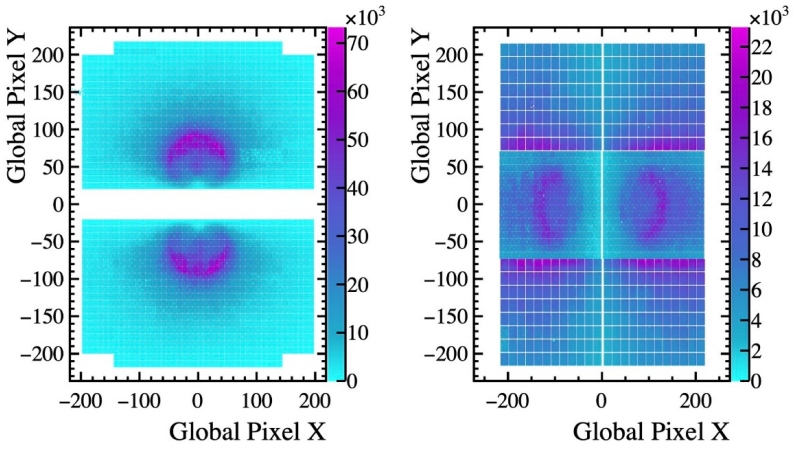


Figure 1: Hitmaps of RICH 1 (left) and RICH 2 (right) during data taking.

The performance of hadron identification in the RICH detectors depends primarily on the number of detected Cherenkov photons per track and on the single-photon Cherenkov angle resolutions. This intrinsic resolution is determined using high-momentum charged particles, as the Cherenkov angle reaches a maximum value for particles with $\beta \approx 1$. The resolution values are extracted from fits to the Cherenkov angle distributions for both RICH 1 and RICH 2. Compared to the Run 2 configuration, an improved resolution is observed, with values close to those predicted by simulation.

3. Calibration and monitoring of the photo-detection chain

While the upgraded RICH detectors were designed to optimise the number of detected Cherenkov photons per track and the single-photon Cherenkov angle resolution, the final performance relies on precise calibrations of the entire photon-detection chain, alignment of all the optical components, and on the long-term operational stability of the system. Continuous and accurate calibration ensures that the timing, gain, and alignment of all components remain within design specifications.

3.1 Background studies

A detailed understanding of background signals is crucial for ensuring optimal photon detection performance. Early tests of the MaPMT showed out-of-time hits, detected with data acquired in an LHC collision scheme with isolated bunches and with a 3 μs-wide acquisition window [5]. These hits are referred to as "Signal Induced Noise" (SIN). The observed timing profile and spatial pattern of SIN events align with photons produced at the MaPMT anode that pass through the mechanical openings around the MaPMT edges, reach the photocathode, generate additional photoelectrons, and are then amplified in the dynode chain, producing delayed signals.
This effect has been fully characterized with a setup that allows the recording of the time spectrum of the noise pulses within 25 ns time-slots [5]. An example of the time distribution of detected signals for different MaPMT high voltage (HV) settings is reported in Figure 2, left. The mean number of SIN pulses is different for each pixel within the MaPMT under study, and for the same pixel between different MaPMT, even if a common pattern of pixels affected by SIN is present. Several

PoS(EPS-HEP2025)518

mitigation strategies have been adopted, including optimisation of the HV settings and tuning of a data acquisition time gate to reject out-of-time hits.

3.2 Hit-rate monitoring

The hit rates of the RICH sub-detectors are continually monitored during LHCb operation. This can also be used to provide a stand-alone luminosity measurement for the LHCb experiment. The luminosity is calibrated during Van der Meer scans, where the separation of the two proton beams is varied in the x and y directions. The luminosity extraction via the measurement of the number of Cherenkov hits (as described in Ref.[6]) can be used to calibrate the RICH MaPMT anode currents, which are sensitive and proportional to the luminosity as displayed in Figure 2, right. The capability to monitor such quantity via the anode currents provides an immediate online estimate of luminosity for the LHCb experiment.

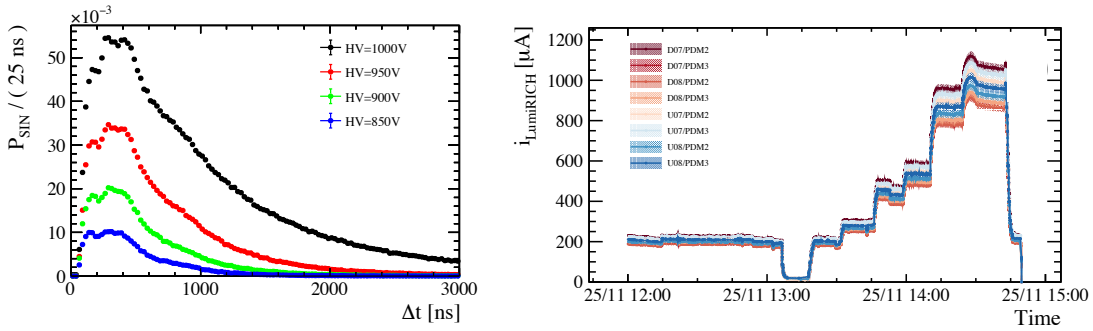


Figure 2: Left: Time distribution of detected events for different MaPMT HV settings [5]. Right: Anode currents variation during a μ scan, where μ is the average number of visible proton-proton interactions per bunch crossing. During a μ scan the average number of visible proton-proton interactions per bunch crossing is varied over time, in order to provide calibration data for the luminosity estimations. The different colors stand for different Photon Detector Modules (defined in Section 3.3) in the high occupancy region of RICH 1 [6].

3.3 Gain equalisation and ageing monitoring

To maximise the single-photon detection efficiency while keeping ageing effects to a minimum, it is essential to account for the difference in gain between different MaPMT. This parameter is determined through dedicated threshold scan measurements, which provide the basis for defining the front-end electronics working points. The same procedure also enables fine adjustment of the HV settings to equalise the detector response and to monitor the ageing of the MaPMT via the gain evolution estimation over time.

During each threshold scan, an integral pulse-height spectrum is recorded for every anode of the RICH detectors (194,560 channels in total). The spectra are fitted with a complementary error function, where the inflection point corresponds to the anode gain expressed in threshold steps. An example is displayed in Figure 3, left. A conversion from threshold steps to physical charge is then obtained through DAC calibration scans.

To equalise the response of the photo-detection planes, the HV settings are derived from the study of the so called "k-factor" curves, which describe the dependence of the MaPMT gain on the

PoS(EPS-HEP2025)518

applied voltage. The gain follows the empirical relation $G = A \cdot \mathrm{HV}^{kn}$, where k depends on the dynode structure and material, and n is the number of dynode stages [7]. The k-factor is evaluated for each MaPMT, but the figure of merit is represented by the average of the gains of all the sensors belonging to a Photon Detector Module (PDM, a collection of sixteen 1-inch MaPMT or four 2-inch MaPMT). This is due to the fact that the HV can be tuned only at the level of the PDMs. An example of a k-factor from one RICH 1 PDM is reported in Figure 3, right. Each PDM k-factor is fitted with a quadratic function, whose inverse relation provides the HV value required to reach a chosen target gain. For RICH 1, this reference gain was set to 1.2 Me^-, corresponding to the typical conditions in the high-occupancy regions of the detector. Applying the resulting HV settings ensures a uniform gain across all photo-detection planes, thus optimising the photon-detection efficiency and overall detector performance.

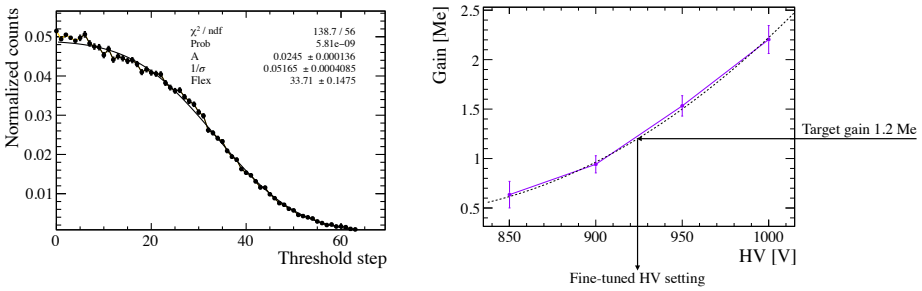


Figure 3: Left: An example of an integral pulse height spectrum for one anode in RICH 1, HV=1000 V. Right: Dependence of gain on the HV setting (k-factor) for a RICH 1 PDM.

Gain monitoring is also important for MaPMT ageing studies, since it is expected at two levels: ageing of the photocathode, implying a loss of quantum efficiency; ageing of the multiplication chain, causing a loss of gain [8]. The gain dependence on HV setting has been compared in two different data-taking periods, as displayed in Figure 4, left: the two k-factor curves are compatible within the relative uncertainties, implying negligible MaPMT ageing. Figure 4, right, reports the PDMs gain distribution across the RICH 1 photo-detection planes extracted with the May 2025 dataset: the gain is still nicely uniform across the different PDMs.

4. Time alignment

During the commissioning phase of Run 3, a key milestone for the RICH system was the implementation of a precise time-alignment procedure between the detector readout and the LHC collisions. After identifying the correct 25 ns time interval of the LHC bunch crossing (coarse time alignment), the RICH detectors can be further time-aligned within this window to ensure optimal signal collection. Simulation studies indicate that the Cherenkov photon signal is contained within a time window of only a few nanoseconds, motivating the development of a fine time-alignment strategy. The output of the CLARO front end ASIC can be sampled eight times between bunch crossings creating eight mini-slots, each 3.125 ns wide, and the signal transition from low to high between mini-slots can be used to accurately detect the arrival time. The readout delays can then be adjusted such that all channels are synchronised within a 6.25 ns window around the mean photon

PoS(EPS-HEP2025)518

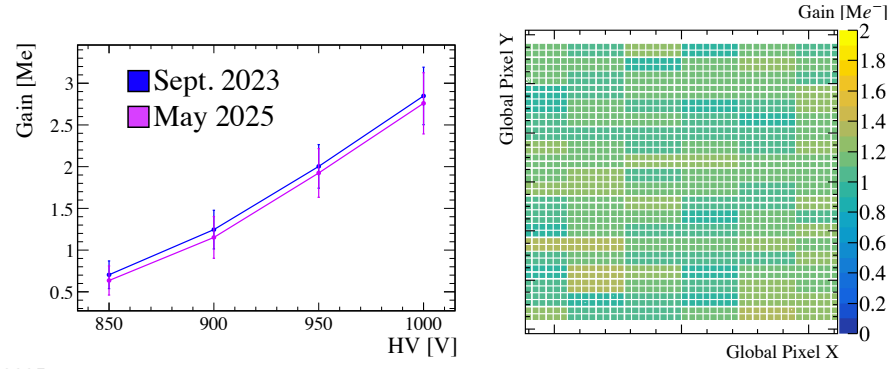


Figure 4: Left: Dependence of gain on the HV setting for a RICH 1 PDM comparing two threshold scan datasets acquired respectively in September 2023 and May 2025. Right: PDM gain distribution expressed in Me^- across the RICH 1 photo-detection planes. The scale shows 44 1-inch MaPMT in the x-axis and 40 1-inch MaPMT in the y-axis.

arrival time. As the time resolution of the CLARO is around 3-4 ns, a smaller gate would reject some of the Cherenkov signal as seen in Figure 5.

The 6.25 ns gating scheme was selected for standard Run 3 operations, ensuring stable and efficient RICH detector performance under higher luminosity conditions.

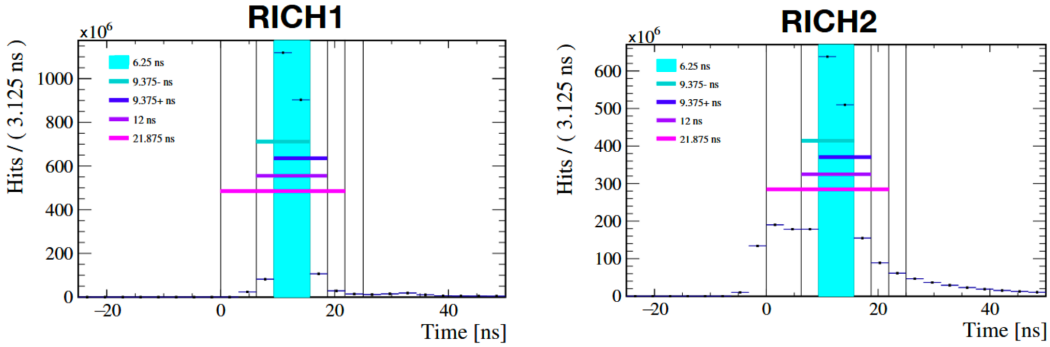


Figure 5: Distribution of the number of hits for RICH 1 (left) and RICH 2 (right) as a function of the signal readout time, binned according to the 3.125 ns readout window. Different gating options are highlighted in different colors.

5. Particle Identification performance

The charged hadron identification performance at LHCb is evaluated using data-driven techniques based on control samples of particles that can be selected purely through kinematic criteria, without relying on the RICH information. Samples of charged pions and kaons are extracted from the decay products of the D^0 meson in the decay chain $D^{*+} \to D^0(\to K^-\pi^+)\pi^+$, while samples of protons are obtained from $\Lambda \to p\pi^-$ [9].

The figure of merit used to quantify the RICH performance is the misidentification rate as a function of the identification efficiency for different charged hadrons. The efficiency of a given

PoS(EPS-HEP2025)518

particle identification (PID) selection applied to a probe hadron (pion, kaon, or proton) is determined through a binned maximum-likelihood fit to the invariant-mass distribution of the parent particle, as displayed in Figure 6, left. This fitting procedure allows the separation of signal and background contributions. The fit is performed both with and without applying the PID selection to the probe particle, and the efficiency is obtained as the ratio of the fitted signal yields in the two cases. By varying the PID selection criteria from loose to tight, one obtains the corresponding efficiency–misidentification profiles. These distributions provide a direct measure of the RICH system's particle-identification performance under realistic experimental conditions. Figure 6, right, displays the comparison of the PID performance obtained in Run 2 and Run 3 in high-multiplicity events. The comparison shows that, even with more visible interactions on average, the upgraded RICH system retains the high-quality charged-hadron identification observed in Run 2 [9].

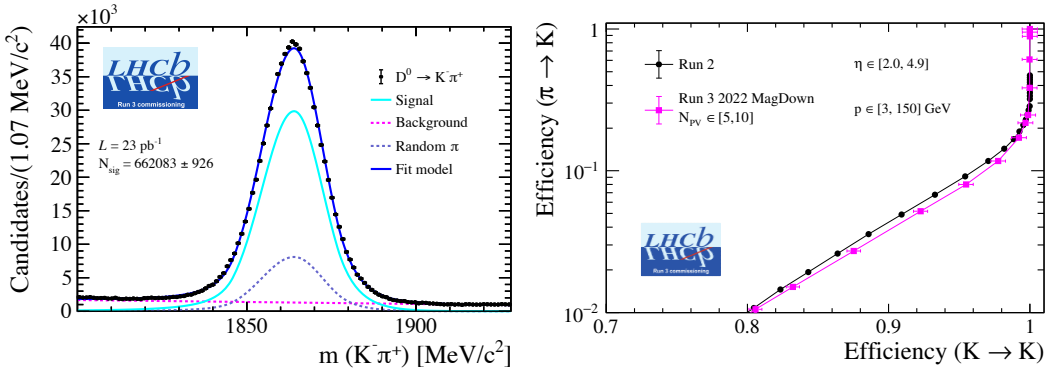


Figure 6: Left: Invariant mass distribution of the $K^-\pi^+$ final state from the D^0 decay. Right: Efficiency of selecting kaons with the associate leakage from misidentifying pions in Run 2 (black) and Run 3 from high multiplicity events (magenta) [9]. Kaons below threshold are identified in pion veto mode.

6. Conclusions

The upgraded LHCb RICH system successfully meets the challenges posed by the five-fold increase in instantaneous LHC luminosity during Run 3, while maintaining stable operation at the full 40 MHz bunch-crossing rate. The upgrade introduces significant improvements in photon detection efficiency through the use of MaPMT and new front-end electronics, supported by precise noise characterisation and mitigation strategies.

The RICH detectors provide charged-hadron identification over an unprecedented momentum range, operating efficiently even under high-occupancy conditions. Since the start of Run 3 data taking, the system has demonstrated excellent stability and performance, exceeding the performance of the previous configuration, and steadily approaches the design values for the single-photon Cherenkov angle resolution. The outstanding performance of the upgraded RICH system ensures robust particle identification capabilities, enabling LHCb to achieve its full physics programme.

PoS(EPS-HEP2025)518

References

[1] R. Aaij et al., *LHCb detector performance*, International Journal of Modern Physics A 30 07 (2015) 1530022, 10.1142/s0217751x15300227

[2] R. Aaij et al., *The LHCb Upgrade I*, JINST 05 (2024) P05065, 10.1088/1748-0221/19/05/p05065

[3] R. Calabrese et al., *Performance of the LHCb RICH detectors during LHC Run 2*, JINST 17 (2022) P07013, 10.1088/1748-0221/17/07/P07013

[4] M. Baszczyk et al., *CLARO: an ASIC for high rate single photon counting with multi-anode photomultipliers*, JINST 12 (2017) P08019, 10.1088/1748-0221/12/08/P08019

[5] M. Andreotti et al., *Characterisation of signal-induced noise in Hamamatsu R11265 Multianode Photomultiplier Tubes*, JINST 16 (2021) P11030, 10.1088/1748-0221/16/11/P11030.

[6] P. Alvarez Cartelle at al., *Luminosity measurement with the LHCb RICH detectors in Run 3*, JINST 20 (2025) P08001, 10.1088/1748-0221/20/08/p08001

[7] HAMAMATSU PHOTONICS K.K., *Photomultiplier tubes, basics and applications*, 2007

[8] M. Calvi et al., *Aging and time resolution measurements for the Hamamatsu R7600 multi-anode photomultiplier tube*, 2011 IEEE Nuclear Science Symposium Conference Record, 10.1109/NSSMIC.2011.6154651

[9] LHCb collaboration, *Charged hadron identification performance with early Run 3 data*, 2023, https://cds.cern.ch/record/2868904

PoS(EPS-HEP2025)518